Journal of Zhejiang University-SCIENCE C (Computers & Electronics)
ISSN 1869-1951 (Print); ISSN 1869-196X (Online)
www.zju.edu.cn/jzus; www.springerlink.com
E-mail: jzus@zju.edu.cn

Hardware design of a localization system for staff in high-risk manufacturing areas*

Rui-rong WANG†, Rong-rong YE, Cui-fei XU, Jian-zhong WANG, An-ke XUE

(*Institute of Information and Control, Hangzhou Dianzi University, Hangzhou 310018, China*)

†E-mail: wangrr@hdu.edu.cn

Received July 21, 2012; Revision accepted Nov. 17, 2012; Crosschecked Dec. 22, 2012

Abstract: In this paper, we propose a hardware design for an effective real time indoor localization system for staff working in high-risk manufacturing areas. Because of the special requirements of our system, the chirp spread spectrum (CSS) is the most suitable indoor localization technology. The details of the new localization system are described. The system involves several anchors, tags, and a gateway, all of which use the nanoLOC TRX transceiver (NA5TR1) RF chip (Nanotron Co., Germany), which is based on the CSS technology. To validate the effectiveness of our system, both ranging and localization tests were carried out. The difference between the ranging accuracy indoors and outdoors was small. The localization system can position indoor mobile staff precisely, enabling the establishment of an emergency rescue mechanism.

Key words: Wireless indoor localization, High-risk manufacturing area, Chirp spread spectrum (CSS), NanoLOC TRX transceiver (NA5TR1)

doi:10.1631/jzus.C1200229 **Document code:** A **CLC number:** TP23

1 Introduction

Some high-risk industries play an important role in China's national development program. However, as accidents have occurred frequently in those industries in recent years, there is growing concern over the safety of staff working in high-risk manufacturing areas (Wang *et al*., 2011). It would be of great assistance to rescuers if the distribution of staff in an accident area could be determined. Therefore, it is necessary to establish an emergency rescue mechanism that includes an indoor localization system.

The system we present in this paper consists of a monitoring center and an indoor localization system. The monitoring center is software on a PC which can display a brief map of the indoor environment and the real-time location of moving staff. The indoor localization system consists of gateways, anchors, and tags. Gateways and anchors are deployed in high-risk manufacturing areas, while tags are carried by moving staff. Anchors calculate their distance from the tags, and then transmit the distance data to gateways that finally send the data to the PC of the monitoring center.

Localization accuracy depends strongly on the quality of the measurements, which are affected by impairments such as network topology, multipath propagation, environmental conditions, interference, noise, and clock drift (Win *et al*., 2011). A range measurement is referred to as a direct path (DP) measurement if it is obtained from a signal traveling along a straight line between two nodes (Conti *et al*., 2012). Due to severe multipath conditions in indoor areas, the estimation of a DP results in small random and sometimes large errors. The small random errors are caused by paths arriving close to the first detected path. The large errors occur when the DP goes below the detection threshold, so the first path detected in

* Project (No. KYH063112027) supported by the Department of Science and Technology of Zhejiang Province, China

the received multipath profile is erroneously considered to be the DP. We refer to these situations as undetected direct path (UDP) conditions, and they can severely degrade the localization accuracy (Alavi and Pahlavan, 2006). Non-line-of-sight (NLOS) propagations, created by physical obstructions in the DP, produce a positive bias in the propagation time and decrease the strength of the received signal, so this is another important negative factor that needs consideration (Shen and Win, 2010). In a situation such as localizing staff working in high-risk manufacturing areas, the presence of the human body also has a large impact, which should not be neglected.

To remove or lessen the effect of these negative factors, we deploy specially to ensure that the tag is in the line of sight of at least three anchors. To achieve this, the anchors in our system are attached to the ceiling of the room with their antennas facing down. The tags, which are carried by moving staff, are also placed as high as possible (in our case, attached to a hat). Moreover, we deploy more anchors than necessary to increase redundancy.

2 Overview

Although the global positioning system (GPS) (Munson and Gupta, 2002; Liu *et al.*, 2007) is the best location-aware system in outdoor environments, it cannot be efficiently used for locating personnel indoors because of signal attenuation. This has led to the study of other indoor localization technologies, such as Wi-Fi (Zhao *et al.*, 2010), radio frequency identification (RFID) (Yu *et al.*, 2009; Tesoriero *et al.*, 2010), ultra-wideband (UWB) (Correal *et al.*, 2003), ZigBee (Goncalo and Helena, 2009), and chirp spread spectrum (CSS) (Wang *et al.*, 2012). Among these technologies, UWB, ZigBee, and CSS are most frequently used to develop indoor localization systems. Because of the special requirements of real time localization of staff in high-risk manufacturing areas, it is important to choose a technology suitable for our system.

2.1 Localization system based on ultra-wideband (UWB)

UWB technology is a viable candidate for enabling accurate localization capabilities through time-of-arrival (TOA) based ranging techniques (Dardari *et al.*, 2009). Such techniques are widely used in high precision radiolocation applications because they achieve high accuracy with centimeter-level ranging resolution (Chu and Ganz, 2005). Their ability to resolve multipath components makes it possible to obtain accurate location estimates without the need for complex estimation algorithms. This precise location estimation capability facilitates many applications such as medical monitoring, security, and asset tracking (Gezici *et al.*, 2005). Fig. 1 shows one of the indoor localization systems based on UWB and developed by the Time Domain Co., USA. The system is called precision location ultra wideband system (PLUS). The constitution of PLUS includes tags, readers, a synchronization distribution panel (SDP), and a location server PC (Fig. 1a). The readers calculate their distance from a tag and then send the distance data to the SDP through a local area network (LAN). In this way, the system can locate a tag with a location accuracy of 15 cm and track 800 tags at one time.

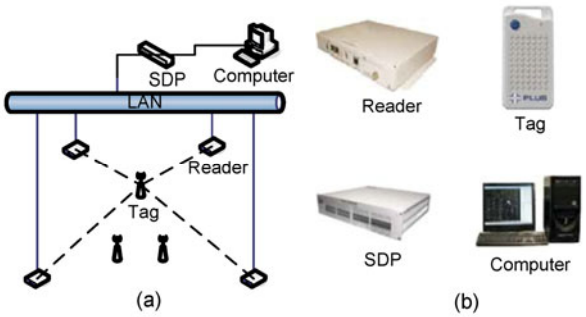

Fig. 1 Structure (a) and products (b) of the precision location ultra wideband system (PLUS) (Time Domain Co., USA)

2.2 Localization system based on ZigBee

ZigBee is a wireless technology well suited for wireless sensor networks (WSNs). The particular superiorities of ZigBee are its convenience for applications, low power consumption, low cost, and ad-hoc network. One of the indoor localization systems based on ZigBee technology is shown in Fig. 2.

The system called MICAZ OEM (Crossbow Co., USA) consists of an anchor tag, a gateway board, and a data collect board. In addition to locating, the system collects the parameters of the environment, such as temperature and humidity.

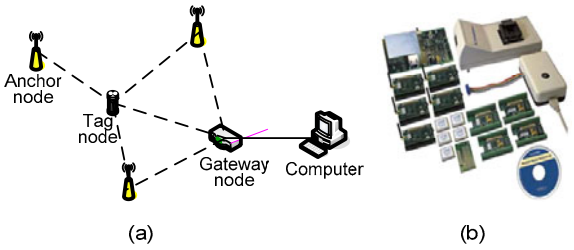

Fig. 2 Structure (a) and products (b) of MICAZ (Crossbow Co., USA)

2.3 Chirp spread spectrum (CSS) technology

CSS is a new radio technology in accordance with the IEEE 802.15.4a (2007) protocol that is an alternative physical layer (PHY) for the IEEE 802.15.4 protocol. It provides highly accurate ranging with low power consumption. The ranging method used by CSS is called symmetrical double-sided two-way ranging (SDS-TWR) (Nanotron Co., Germany) (Yoon and Cha, 2011). During the first round of measurement, node 1 sends a data packet to node 2 that returns a hardware acknowledgement (Fig. 3). Meanwhile, node 1 records the propagation delay T_1, which covers the whole process of the first round, and node 2 records the processing delay T_2, which starts from the receiving of the data packet and ends with the sending of the acknowledgement. During the second round of measurement, this process is repeated. However, the process begins with node 2 and the data packet contains T_2. The propagation delay is marked as T_3 and the processing delay as T_4. Finally, node 2 sends the data packet containing T_3 to node 1 which calculates the distance using the data recorded as above. The equation used to calculate distance is given as

$$d=\frac{c(T_1-T_2+T_3-T_4)}{4}, \tag{1}$$

where d denotes the distance between nodes 1 and 2, and c is the speed of light.

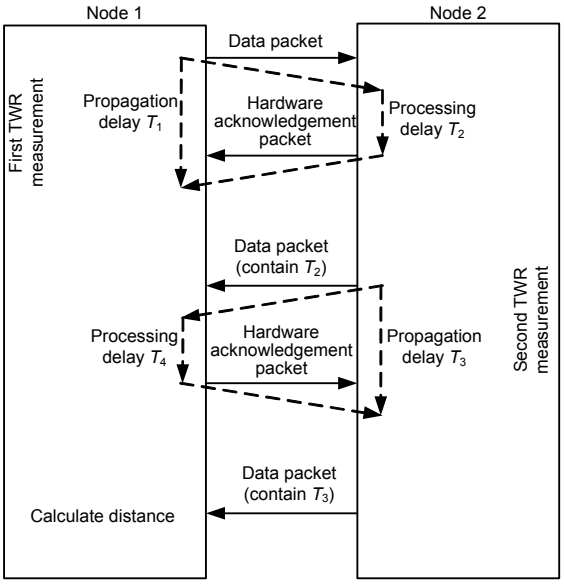

Fig. 3 Process of symmetrical double-sided two-way ranging (SDS-TWR)

2.4 Comparison of ultra-wideband (UWB), ZigBee, and chirp spread spectrum (CSS)

A system specifically designed for localization of staff in high-risk manufacturing areas must be reliable as well as practical. As the victims to be rescued need to be in sight of the rescuers, the accuracy should be less than 1.5 m. The power consumption must be low enough so that the rescue will not be interrupted by a power shortage. The size and weight of the nodes, especially the tag, should be as small as possible for the convenience of carry. Moreover, the cost of the system should not be so high as to hinder its use in high-risk manufacturing areas.

The performance of UWB, ZigBee, and CSS was compared (Table 1) to determine the technology most suitable for application in our system. Although UWB has the highest accuracy, it is too expensive for a localization system based on UWB to be widely used. The accuracy of CSS is higher than that of ZigBee but lower than that of UWB. However, it is not necessary

Table 1 Comparison of ultra-wideband (UWB), ZigBee, and chirp spread spectrum (CSS)

Technology	Standard	Transmission range (m)	Accuracy (m)	Power consumption	Rate (bps)	Band (Hz)	Price
UWB	IEEE 802.15.3a	200	0.1	Ultra low	100 M–1 G	3.1–10.6 G	High
ZigBee	IEEE 802.15.4	300	>3	Low	250 k	2.4 G	Low
CSS	IEEE 802.15.4a	300	<1	Ultra low	125 k–2 M	2.4 G	Low

for the localization system to have the highest accuracy, as in emergency rescue situations, rescuers can find victims as long as they are in sight. Therefore, a CSS with an accuracy of less than 1 m is sufficient. Power consumption is another important parameter of the system because the power supply of a tag comes from a battery and it is inconvenient to have to change the battery. Thus, the low power consumption of CSS is another advantage compared with ZigBee. CSS technology is the most suitable solution for real time localization of staff in high-risk manufacturing areas, owing to its high accuracy, low power consumption, and low price.

3 Hardware developments

The indoor localization system adopts the structure shown in Fig. 4. The system includes three node types: anchors, tags, and gateways. As the tags need to be carried by the moving staff, they should be as small as possible. The gateway needs to communicate with the computer, so it should include extra connectors.

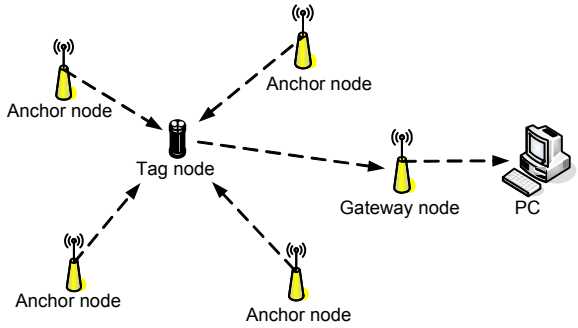

Fig. 4 Structure of the system based on chirp spread spectrum (CSS)

3.1 Circuit design of the anchor and gateway

For circuit design of localization nodes whose ranging measurement uses CSS technology, we chose the nanoLOC TRX transceiver (NA5TR1) (Nanotron Co., Germany). The average ranging accuracy of NA5TR1 is 2 m indoors and 1 m outdoors.

NA5TR1 requires two quartz crystal oscillators with a frequency of 32 MHz and 32.768 kHz respectively, whose circuits are shown in Fig. 5. The 32-MHz quartz crystal is used for baseband control, radio control, and other baseband use, while the 32.768-kHz quartz crystal is used for running the real time clock and power management. To obtain a high ranging accuracy, the standard clock of the baseband must be stable, so a Pierce-type crystal is used for the oscillator of the baseband (Hur and Ahn, 2010).

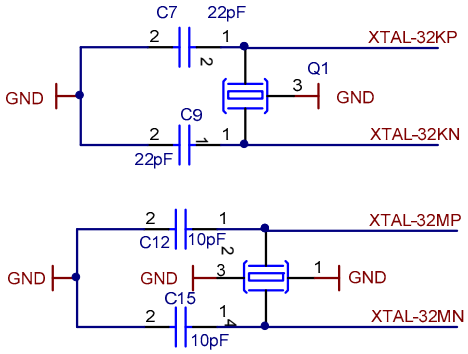

Fig. 5 Quartz crystal oscillator circuits

ATmega128A is used as the microcontroller that governs the operation of the NA5TR1. The ATmega128A is an 8-bit microcontroller with 2.7–5.5 V operating voltage and an in-system programmable flash of 128 KB, achieving a high performance with low power consumption. The ATmega128A has six sleep modes: idle, analog to digital converter (ADC) noise reduction, power-save, power-down, standby, and extended standby. These enable large reductions in power consumption.

As the NA5TR1 needs to convert an unbalanced signal into a balanced signal, a converter called balanced to unbalanced (BALUN) (Würth Elektronik GmbH & Co. KG, Germany) is used. After the conversion, a bandpass filter blocks the signals outside the bandwidth of CSS signals. The high-cutoff-frequency of the bandpass filter is selected as 2.5 GHz, and the low-cutoff-frequency as 2.4 GHz. The circuit design of the radio frequency (RF) transmitter and receiver is shown in Fig. 6.

To communicate with the computer, the nodes include an RS232 bus interface. The circuit (Fig. 7) includes capacitances and an RS232 bus driver, which provides a mutual conversion function between the RS232C and the transistor-transistor logic (TTL) level. As I/O voltage is different between ATmega128A and NA5TR1, TI's SN74AVC4T245 4-bit

dual-supply bus transceiver is used. This supports partial power-down-mode operation to reduce power consumption and has a maximum data rate of up to 200 Mbps when translated into 2.5 V.

The power is supplied by two AA-type batteries (Fig. 8). NCP1402, a micropower switching regulator, is used to convert the battery power of under 3.0–3.3 V for the input of the ATmega128A microcontroller. As NA5TR1 requires 2.5 V rather than 3.3 V, the power is regulated by TPS79425, a low dropout voltage regulator that can minimize noise as it has no switching operation.

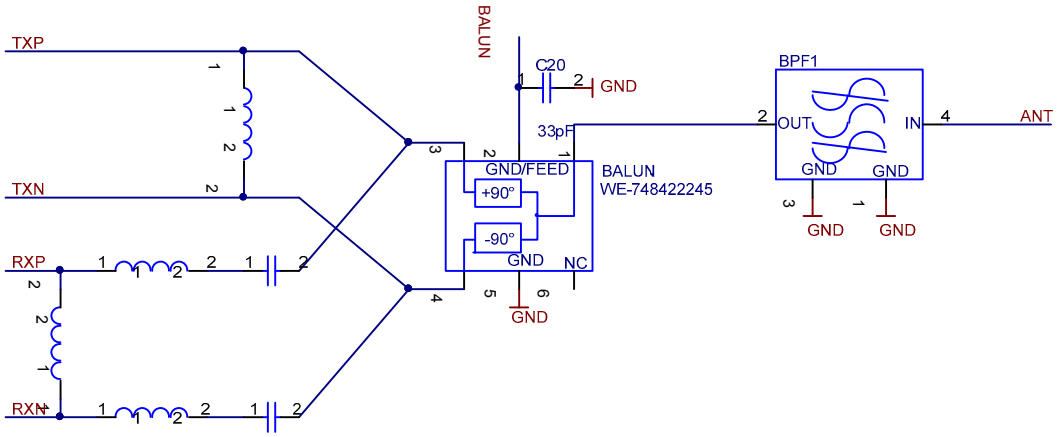

Fig. 6 Radio frequency (RF) transmitter and receiver circuit

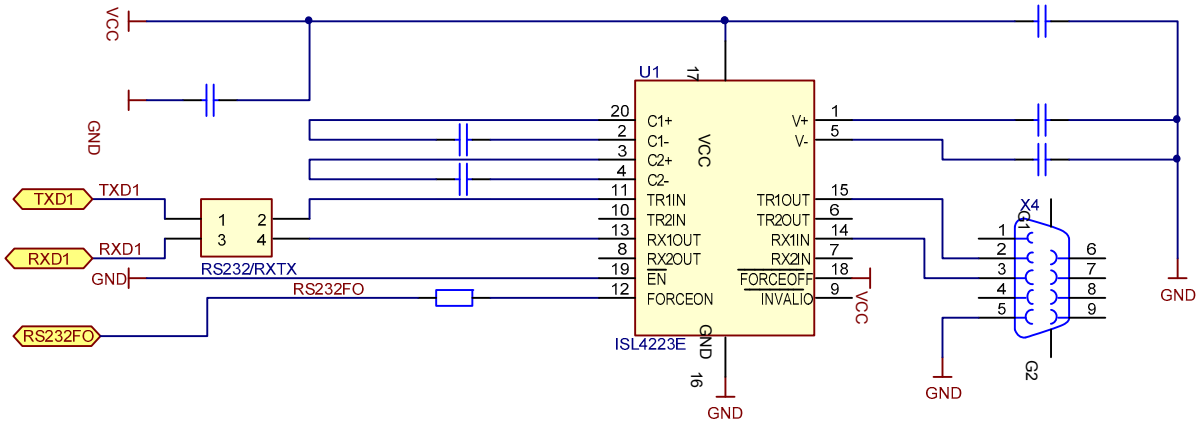

Fig. 7 RS232 bus interface circuit

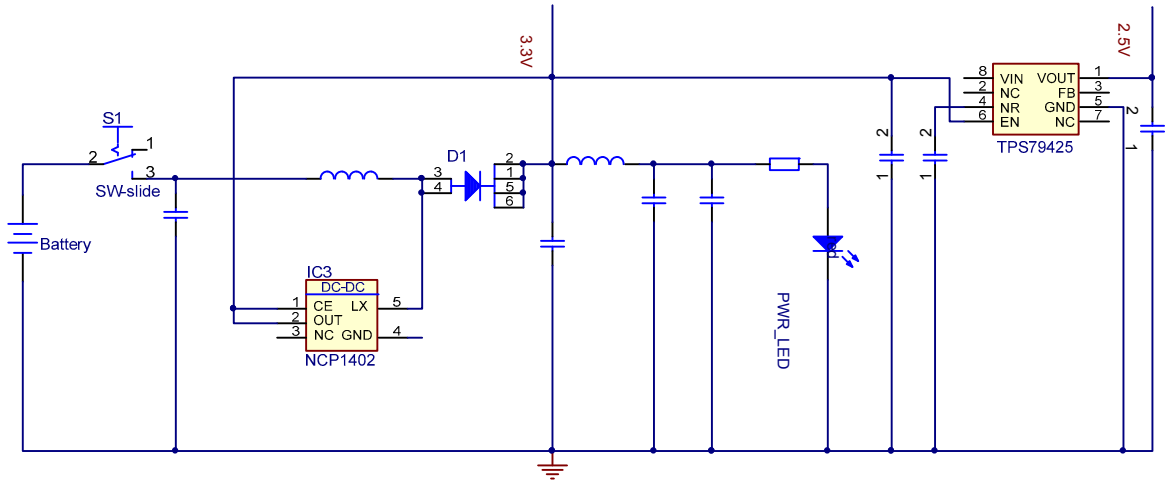

Fig. 8 Power supply circuit

3.2 Circuit design of the tag

The tag uses ATmega644V as the microcontroller, which also achieves high performance with low power consumption. It is an 8-bit microcontroller which requires 1.8–5.5 V operating voltage when its speed is lower than 4 MHz. ATmega644V can use the same voltage input as NA5TR1 and also has six sleep modes: idle, ADC noise reduction, power-save, power-down, standby, and extended standby. Its power consumption is lower than that of ATmega128A.

Surface mount assembly (SMA) or surface mounted device (SMD) antennas are chosen in different circumstances to minimize the size of the tag. When an SMA antenna is chosen, the antenna circuit is as shown in Fig. 9. An SMA antenna has a higher gain than an SMD antenna, but it is much larger.

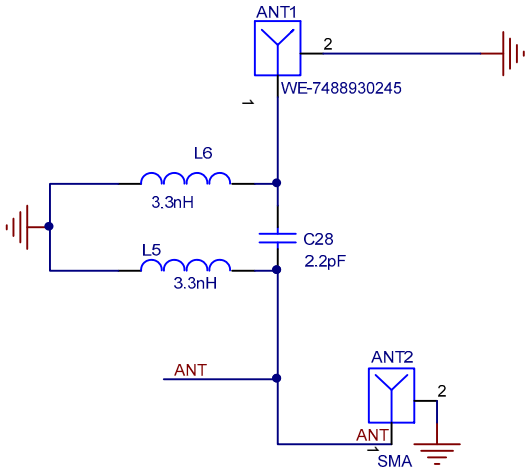

Fig. 9 Antenna circuit

3.3 Design of printed circuit board (PCB) and balanced to unbalanced (BALUN)

The PCB of the nodes is divided into two parts, the RF and the power parts. The RF part contains NA5TR1 and the microcontroller, while the power part supplies power and connectors to the RF part. The design minimizes the size of the nodes, especially the size of the tags. There are two kinds of power part: one supplies power only to the RF part and can be very small, and the other supplies both power and connectors to the RF part. The design also reduces the cost of the system, as the PCB of the RF part consists of four layers and the PCB of the power part consists of two layers. Though 2-layer PCBs cost less, the signal traces have to share the power and the ground plane. In contrast, 4-layer PCBs make a stable return path and ground bounce by their steady distribution of the power/ground plane compared with 2-layer PCBs (Wu *et al*., 2002).

BALUN can not only convert the signal from balance to unbalance or vice versa, but also convert the impedance from 200 to 50 Ω or vice versa. So, the width of the line connected to BALUN should be designed to provide proper impedance-matching characteristics. The calculation of impedance on a microstrip line is shown as

$$Z_0 \approx \frac{87}{\sqrt{\varepsilon_r + 1.41}} \ln\left(\frac{5.98h}{0.8w + t}\right), \tag{2}$$

where Z_0 indicates the impedance (Ω), ε_r is the dielectric constant, h is the height between the line and the substrate (m), w is the width of the line (m), and t is the thickness of the line (m).

Eq. (2) can be turned to

$$w \approx \exp\left(\frac{5.98h}{Z_0\sqrt{\varepsilon_r + 1.41}/87} - t\right) \Big/ 0.8. \tag{3}$$

To obtain a more accurate width of the line, Polar Si9000 is used. The interface of Polar Si9000 and the parameters is shown in Fig. 10. The width of the lower line (W1) and the width of the upper line (W2) are calculated as

$$W1 = w + 0.5, \tag{4}$$

$$W2 = w - 0.5. \tag{5}$$

The values of these parameters depend on the material of the PCB, its manufacturing process, and the characteristics of BALUN. In our design, the material used is FR-4 whose dielectric constant is 4.6. The dielectric constant of the coating above the substrate and trace is 4. The impedance is 50 Ω and other parameters are as offered by the manufacturer. According to Eq. (3), the result is w=12.8658 m, while after modification by Polar Si9000, the result is w=12.0583 m. The width of the line is chosen as 12 m. The calculation of impedance is shown in Fig. 11.

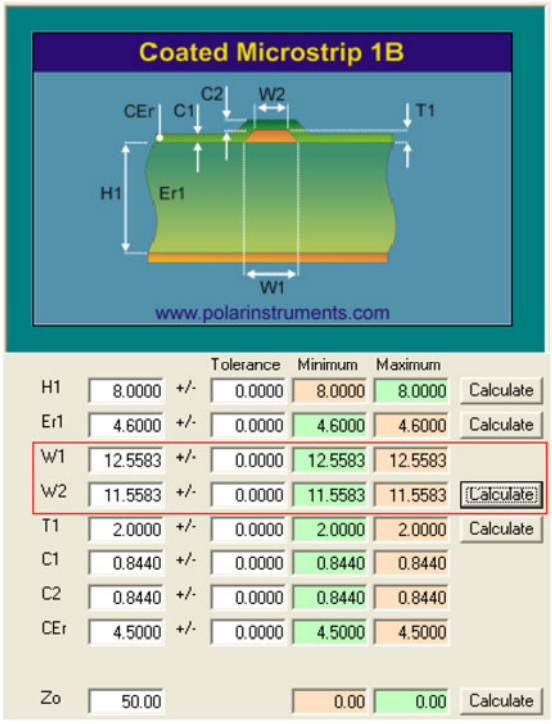

Fig. 10 Calculating the width with Polar Si9000

Z_0: impedance (Ω); Er1: dielectric constant; H1: height between the line and the substrate (m); T1: thickness of the line (m); C1: thickness of the coating above the substrate (m); C2: thickness of the coating above the trace (m); CEr: coating dielectric; W1: width of the lower line (m); W2: width of the upper line (m)

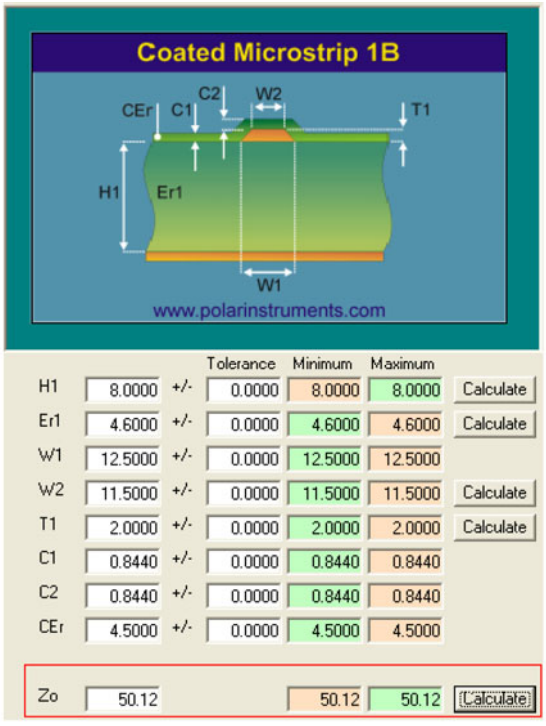

Fig. 11 Calculating the impedance with Polar Si9000

3.4 End products of nodes

Fig. 12a shows the end products of the anchor and gateway, whose power can be supplied by two AA-type batteries and a power adapter. Fig. 12b shows the end product of a tag. The board at the top left is the RF part and the board at the top right is the power supply of the RF part without a programmable connector; the power is supplied by a 3-V lithium cell to minimize the size. The board at the bottom is the power supply of the RF part with a programmable connector which uses two AA-type batteries or a power adapter as its power supply.

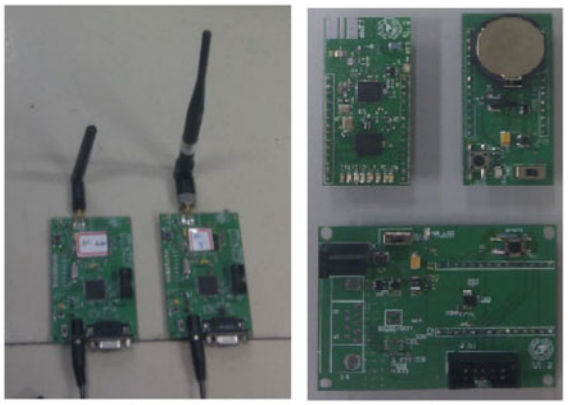

Fig. 12 End products of the anchor and gateway (a) and a tag (b)

4 Experiments

4.1 Ranging test

Before localization, we tested the ranging accuracy of the nodes. The nodes were placed indoors and outdoors to compare the performance. The distance between the anchor and the tag was chosen as 5, 10, 15, and 20 m, and the distance was measured 100 times for each. The indoor environment was a corridor of Laboratory Building 2 of Hangzhou Dianzi University (Hangzhou, China), whose cross section is about 3 m×3 m. As the ceiling and the wall reflect the RF signal, the ranging accuracy would be affected. The outdoor environment was an open area outside the same laboratory building. Without the unfavorable reflection, the accuracy was comparatively high.

Fig. 13 depicts the measured distance and Table 2 shows the ranging error. The environment

where we conducted the experiment is shown in Fig. 14. Although the accuracy of the indoor ranging was lower than that of the outdoor ranging, the difference was small. The ranging accuracy of CSS is less than 1 m in theory, but the result of the experiment indicates that the ranging accuracy of the system is more than 1 m in practical applications.

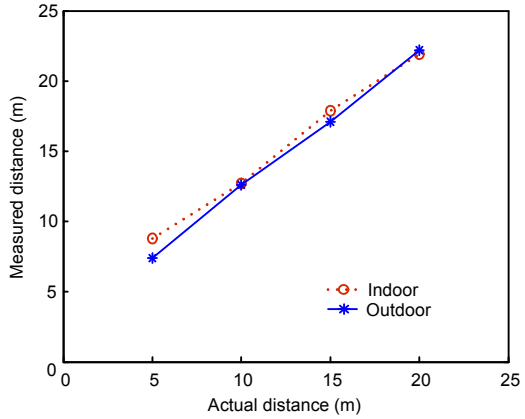

Fig. 13 Measured distances in the experiments

Table 2 Error of ranging test

Actual distance (m)	Indoor (m)	Outdoor (m)
5	3.8	2.4
10	2.7	2.6
15	2.9	2.1
20	1.9	2.2

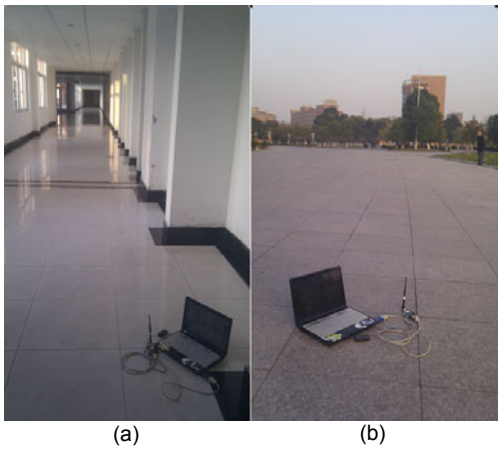

Fig. 14 Experiment environment: (a) Indoor; (b) Outdoor

4.2 Localization test

4.2.1 Localization algorithm

The localization algorithm we applied to test the effectiveness of our design was maximum likelihood estimation, which estimates the position of a tag by minimizing the difference between the measuring distance and the estimated distance. The positions of the anchors were known and marked as (x_1, y_1), (x_2, y_2), …, (x_n, y_n), while the distances between the anchors and the tag were measured and marked as d_1, d_2, …, d_n. If all the above information is accurate, the coordinates of the tag marked (x_o, y_o) should satisfy

$$\begin{cases} (x-x_1)^2+(y-y_1)^2=d_1^2, \\ (x-x_2)^2+(y-y_2)^2=d_2^2, \\ \quad\vdots \\ (x-x_n)^2+(y-y_n)^2=d_n^2. \end{cases} \tag{6}$$

However, because in practical applications the information cannot be accurate and contains errors, there is no solution to the above formula. So, minimum mean square estimation was employed to obtain the optimal estimated position $(\hat{x}_o, \hat{y}_o)$ as follows:

$$(\hat{x}_o, \hat{y}_o)=\arg\min\sum_{i=1}^{n}\left(\sqrt{(x_i-x_o)^2+(y_i-y_o)^2}-d_i\right)^2. \tag{7}$$

According to Eq. (7), we can deduce that the coordinates of the tag can be calculated using

$$(\hat{x}_o, \hat{y}_o)=(\boldsymbol{A}^{\mathrm{T}}\boldsymbol{A})^{-1}\boldsymbol{A}^{\mathrm{T}}\boldsymbol{B}, \tag{8}$$

where

$$\boldsymbol{A}=\begin{bmatrix} 2(x_1-x_n) & 2(y_1-y_n) \\ 2(x_2-x_n) & 2(y_2-y_n) \\ \vdots & \vdots \\ 2(x_{n-1}-x_n) & 2(y_{n-1}-y_n) \end{bmatrix}, \tag{9}$$

$$\boldsymbol{B}=\begin{bmatrix} x_1^2+y_1^2-x_n^2-y_n^2+d_n^2-d_1^2 \\ x_2^2+y_2^2-x_n^2-y_n^2+d_n^2-d_1^2 \\ \vdots \\ x_{n-1}^2+y_{n-1}^2-x_n^2-y_n^2+d_n^2-d_{n-1}^2 \end{bmatrix}. \tag{10}$$

4.2.2 Localization result

The software called LocClient, which we used as the monitoring center, is shown in Fig. 15. To show the localization result clearly, it imports a map and

sets the coordinates of four anchors at the four corners of the user interface before it displays the real-time and history coordinates of the moving tag. There are two kinds of LocClient interface: one displays the moving track as in Fig. 15a while the other displays the real-time position of moving staff as in Fig. 15b. The four red points denote four anchors installed in the area, while the blue points in Fig. 15a mark the moving track of the tag, and the black point in Fig. 15b is the current position of the tag.

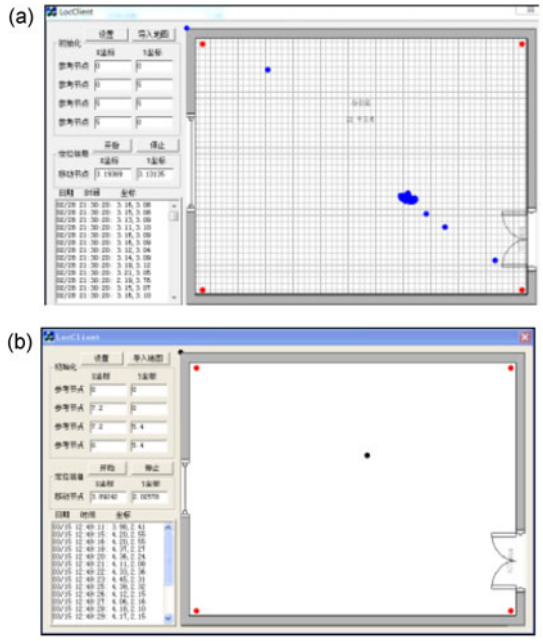

Fig. 15 Monitoring center: interface with (a) and without (b) moving track

The four red points denote four anchors installed in the area, while the blue points in (a) mark the moving track of the tag, and the black point in (b) is the current position of the tag. References to color refer to the online version of this figure

The experiments were carried out at the Institute of Information and Control of Hangzhou Dianzi University. The deployment of the indoor localization system is shown in Fig. 16. The size of the room is about 6 m×10 m. The anchors were placed at the four corners of the room, slightly below the ceiling. As there were not many barriers in the room, placing the anchors on the floor or on the desk would not affect the localization process too much. Placing the nodes high better simulates high-risk manufacturing areas, as the nodes need to be placed without affecting the normal operations in real applications. The localization errors found in our experiment are shown in Table 3.

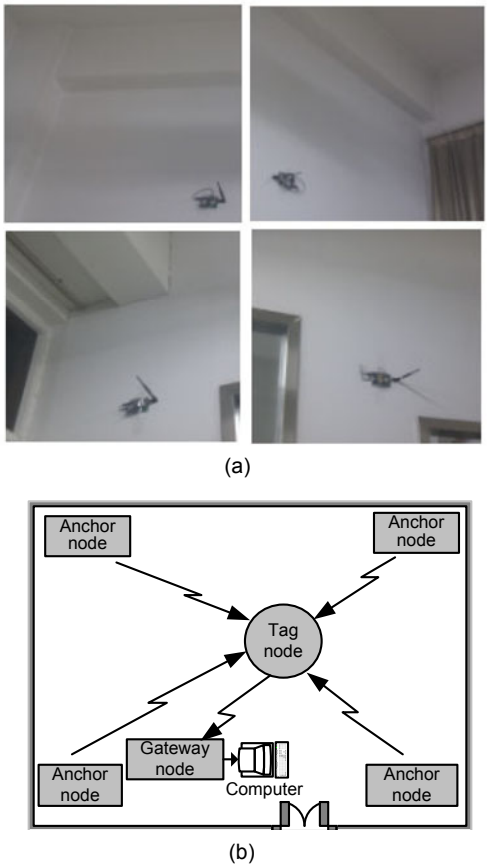

Fig. 16 Deployment of the indoor localization system

(a) Test environment at the Institute of Information and Control of Hangzhou Dianzi University (Hangzhou, China); (b) Sketch map of system

Table 3 Errors of the indoor localization test

Real position (m)		Localization result (m)		Error (m)
X	*Y*	*X*	*Y*	
1	1	2.61	2.96	2.54
2	7	1.21	3.38	3.70
3	5	3.97	4.19	1.26
4	4	3.65	6.09	2.12
4	3	5.98	1.32	2.60
5	8	5.69	9.37	1.53

5 Conclusions

We designed an indoor localization system that attempts to meet the needs of an effective real-time indoor localization system for staff working in high-risk manufacturing areas. To achieve this aim, we chose CSS technology, which can achieve a high

ranging accuracy and uses a tag small enough to be carried by staff in high-risk areas. We describe the hardware design of the new localization system in great detail. We conducted experiments to validate the effectiveness of our system. The results proved that the system performs well in indoor localization, making it suitable for the establishment of an emergency rescue mechanism.

References

Alavi, B., Pahlavan, K., 2006. Modeling of the TOA-based distance measurement error using UWB indoor radio measurements. *IEEE Commun. Lett.*, **10**(4):275-277. [doi:10.1109/LCOMM.2006.1613745]

Chu, Y.C., Ganz, A., 2005. A UWB-Based 3D Location System for Indoor Environments. 2nd Int. Conf. on Broadband Networks, p.1147-1155. [doi:10.1109/ICBN.2005.1589737]

Conti, A., Guerra, M., Dardari, D., Decarli, N., Win, M.Z., 2012. Network experimentation for cooperative localization. *IEEE J. Sel. Areas Commun.*, **30**(2):467-475. [doi:10.1109/JSAC.2012.120227]

Correal, N.S., Kyperountas, S., Shi, Q., Welborn, M., 2003. An UWB Relative Location System. IEEE Conf. on Ultra Wideband Systems and Technologies, p.394-397. [doi:10.1109/UWBST.2003.1267871]

Dardari, D., Conti, A., Ferner, U., Giorgetti, A., Win, M.Z., 2009. Ranging with ultrawide bandwidth signals in multipath environments. *Proc. IEEE*, **97**(2):404-426. [doi:10.1109/JPROC.2008.2008846]

Gezici, S., Zhi, T., Giannakis, G.B., Kobayashi, H., Molisch, A.F., Poor, H.V., Sahinoglu, Z., 2005. Localization via ultra-wideband radios: a look at positioning aspects for future sensor networks. *IEEE Signal Process. Mag.*, **22**(4):70-84. [doi:10.1109/MSP.2005.1458289]

Goncalo, G., Helena, S., 2009. Indoor Location System Using ZigBee Technology. 3rd Int. Conf. on Sensor Technologies and Applications, p.152-157. [doi:10.1109/SENSORCOMM.2009.31]

Hur, H., Ahn, H.S., 2010. A circuit design for ranging measurement using chirp spread spectrum waveform. *IEEE Sens. J.*, **10**(11):1774-1778. [doi:10.1109/JSEN.2010.2049488]

IEEE 802.15.4a, 2007. Part 15.4: Wireless Medium Access Control (MAC) and Physical Layer (PHY) Specification for Low-Rate Wireless Personal Area Networks (LRWPANs): Amendment to Add Alternative PHY.

Liu, H., Drabi, H., Banerjee, P., Liu, J., 2007. Survey of wireless indoor positioning techniques and systems. *IEEE Trans. Syst. Man Cybern.*, **37**(6):1067-1080. [doi:10.1109/TSMCC.2007.905750]

Munson, J.P., Gupta, V.K., 2002. Location-Based Notification as a General-Purpose Services. Proc. 2nd Int. Conf. on Mobile Commerce, p.40-44. [doi:10.1145/570705.570713]

Shen, Y., Win, M.Z., 2010. Fundamental limits of wideband localization-Part I: A general framework. *IEEE Trans. Inf. Theory*, **56**(10):4956-4980. [doi:10.1109/TIT.2010.2060110]

Tesoriero, R., Tebar, R., Gallud, J.A., Lozano, M.D., Penichet, V.M.R., 2010. Improving location awareness in indoor spaces using RFID technology. *Expert Syst. Appl.*, **37**(1):894-898. [doi:10.1016/j.eswa.2009.05.062]

Wang, J., Gao, Q.H., Yu, Y., Wang, H.Y., Jin, M.L., 2012. Toward robust indoor localization based on Bayesian filter using chirp-spread-spectrum ranging. *IEEE Trans. Ind. Electr.*, **59**(3):1622-1629. [doi:10.1109/TIE.2011.2165462]

Wang, R.R., Zhang, Z.Y., Wang, J.Z., Xue, A.K., 2011. A New Solutions for Staff Localization in Chemical Plan. Proc. Int. Conf. on System Science and Engineering, p.503-508. [doi:10.1109/ICSSE.2011.5961955]

Win, M.Z., Conti, A., Mazuelas, S., Yuan, S., Gifford, W.M., Dardari, D., Chiani, M., 2011. Network localization and navigation via cooperation. *IEEE Commun. Mag.*, **49**(5):56-62. [doi:10.1109/MCOM.2011.5762798]

Wu, C.T., Shiue, G.H., Lin, S.M., Wu, R.B., 2002. Composite effects of reflections and ground bounce for signal line through a split power plane. *IEEE Trans. Adv. Pack.*, **25**(2):297-301. [doi:10.1109/TADVP.2002.803263]

Yoon, C., Cha, H., 2011. Experimental analysis of IEEE 802.15.4a CSS ranging and its implications. *Comput. Commun.*, **34**(11):1361-1374. [doi:10.1016/j.comcom.2011.02.002]

Yu, K.M., Lee, M.G., Liao, C.T., Lin, H.J., 2009. Design and Implementation of a RFID Based Real-Time Location-Aware System in Clean Room. IEEE Int. Symp. on Parallel and Distributed Processing with Applications, p.382-388. [doi:10.1109/ISPA.2009.84]

Zhao, M., Yang, H., Liu, J.F., Chen, Y.Q., Zhou, J.Y., 2010. Directional Wi-Fi Based Indoor Location System for Emergency. Ubiquitous Intelligence & Computing and 7th Int. Conf. on Autonomic & Trusted Computing, p.501-502. [doi:10.1109/UIC-ATC.2010.53]